

The effect of lanthanum substitution on the ferroelectric and piezoelectric properties of $(\text{Pb}_{0.88}\text{Sr}_{0.12})(\text{Zr}_{0.54}\text{Ti}_{0.44}\text{Sb}_{0.02})\text{O}_3$ ceramics

H. Goudarzi¹, S. Baghshahi^{1*}, R. Tabarzadi²

¹ Department of Materials Science and Engineering, School of Engineering, Imam Khomeini International University, Qazvin, Iran

² Department of Ceramic Engineering, Material and Energy Research Centre, Alborz, Iran

Abstract

Piezoelectric ceramics based on lead zirconate titanate (PZT) with a composition of $(\text{Pb}_{0.88-3x/2}\text{Sr}_{0.12}\text{La}_x)(\text{Zr}_{0.54}\text{Ti}_{0.44}\text{Sb}_{0.02})\text{O}_3$ where $x=0.0, 0.005$ and 0.01 were synthesized using conventional solid state sintering at 1280°C . The effect of lanthanum substitution on the microstructure, ferroelectric and piezoelectric properties of the samples was studied. The results showed that lanthanum substitution was beneficial for densification of the samples during sintering and the samples with 1.0 mol% lanthanum exhibited the maximum density of 7340 Kg.m^{-3} when sintered at 1280°C . Moreover, the piezoelectric coefficient (d_{33}), relative dielectric constant (ϵ_r), dielectric loss ($\tan\delta$), electromechanical coupling coefficient (k_p) and the Curie temperature (T_C) of the samples reached the optimal values of 635 pC/N, 3000, 0.018, 0.67 and 195°C respectively at 0.5 mol% lanthanum substitution. Furthermore, the bulk density (ρ) was 7310 Kg.m^{-3} for the same sample. The results indicate that the lanthanum doped PSZTS ceramics can be hopefully used in applications such as pulsed transmitting transducers, high sensitivity receivers and actuators with large displacements.

Keywords: PSZTS; Lanthanum additive; ferroelectric and piezoelectric properties;

1. Introduction

PZT ceramics may often be modified with the introducing donor and acceptor additives to create 'soft' and 'hard' PZT materials [1–3]. PZT and modified PZT with acceptors and donors have important technological applications as transducers, detectors and for actuators [4, 5]. It has been reported that the high ferroelectric and piezoelectric properties of PZT with the Perovskite type structure (general formula ABO_3) have been observed for compositions near the morphotropic phase boundary (MPB) where the Zr/Ti ratio is 52:48 at room temperature. Most commercial ferroelectric ceramics have thus been designed in the vicinity of the MPB with various forms of doping in order to achieve improved properties [2, 3] For example, ions of alkaline-earth metals, e.g. Sr^{2+} , Ca^{2+} and Ba^{2+} have frequently been used to substitute for Pb^{2+} [6, 7]. Zheng et al. [7] reported that Sr-modified PZT ceramics generally have higher dielectric and piezoelectric properties than pure PZT. Such Sr substitutions on the A-site in PZT ceramics tend to shift the MPB composition towards the tetragonal phase. The piezoelectric coefficient can then be optimized for the tetragonal phase field close to but not exactly at the MPB.

A great deal of effort has been made during the last decades to reduce the sintering temperature of PZT, while retaining proper ferroelectric and piezoelectric properties. Through these efforts, many dopants have been examined for enhancing densification and improving performance. In particular, donor dopants such as Nb^{5+} [8, 9], W^{6+} [10], Sb^{5+} [11], and La^{3+} [12–14] have been widely investigated due to their significant influence on defect chemistry and domain engineering. Among these, Nb-based

1 modifications have also been reported in our previous study [8], which provides a
2 relevant comparison framework for understanding donor-doping effects in similar PZT-
3 based systems. Up to now, however, research on the La-doped
4 $(\text{Pb}_{0.88}\text{Sr}_{0.12})(\text{Zr}_{0.54}\text{Ti}_{0.44}\text{Sb}_{0.02})\text{O}_3$ (PSZTS) ceramics adapted from Zheng et al. [7] has
5 rarely been reported.

6 In this study, La^{3+} substitution introduces two important effects: (i) a “volume effect”
7 arising from the ionic size mismatch between La^{3+} and Pb^{2+} , leading to slight lattice
8 contraction and structural modification, and (ii) a “charge effect” associated with
9 aliovalent substitution, which induces Pb vacancies for charge compensation and
10 influences densification and electrical properties.

11 2. Experimental

12 The samples with the general formula $(\text{Pb}_{0.88-3x/2}\text{Sr}_{0.12}\text{La}_x)(\text{Zr}_{0.54}\text{Ti}_{0.44}\text{Sb}_{0.02})\text{O}_3$ where x
13 was 0, 0.5 and 1.0 mol%, respectively, were fabricated using the solid state method
14 with the related oxide powders. The raw materials were all oxide powders of analytical
15 grade. These powders were mixed and milled in planetary fast mill, with a zirconia jar
16 ($V=250\text{ cm}^3$) and balls ($d=15\text{ mm}$). The ball-to-powder weight ratio was 15:1, powder
17 quantity was 40 g, milling speed was 300 rpm and milling time was 20 min. Distilled
18 water was used as the media. The suspensions were dried and calcined at 850°C for 2
19 h, at a heating rate of $2^\circ\text{C}/\text{min}$ and a cooling rate of $5^\circ\text{C}/\text{min}$. The calcined powders
20 were then ball-milled again for 20 min to crush the agglomerates and achieve a
21 submicron particle size distribution.

22 After granulation using a solution of polyvinyl alcohol as a binder, the as-synthesized
23 samples were uniaxially pressed into disks of 30 mm diameter and about 4 mm
24 thickness at a pressure of 150 MPa. Binder was removed by soaking the disks at 550°C
25 for 3 h. Following binder burnout, the green compacts were sintered at 1280°C for 1 h
26 in sealed alumina crucibles and the heating and cooling rates were $3^\circ\text{C}/\text{min}$ and
27 $5^\circ\text{C}/\text{min}$, respectively. During the sintering process at 1280°C , PbZrO_3 (PZ) powder
28 was used as the PbO-rich atmosphere buffer to minimize lead volatilization. . The
29 sintered samples were polished and lapped to 3 mm thickness and fired-on silver paste
30 was applied to both surfaces of the samples as electrodes. The ceramic samples were
31 polarized under a direct current field of 2 KV/mm at 120°C in a silicone oil bath for 20
32 min.

33 The bulk density of the sintered samples was measured by the Archimedes' method
34 using water. The crystal structure of the calcined powders was analyzed using an X-ray
35 diffractometer (XRD, PANalytical-Model XPert PRO MPD). The microstructure was
36 investigated with a Field emission scanning electron microscope (FESEM, Model
37 MIRA 3 LMU\TESCAN). The dielectric properties were studied by measuring the
38 capacitance and dielectric loss at 1 kHz at the room temperature using an impedance-
39 gain analyzer (IGA, Model HP4194A). Dielectric constant was computed using the
40 specimen dimensions and the vacuum permittivity ($\epsilon_0=8.854\times 10^{-12}\text{ F.m}^{-1}$). The
41 piezoelectric constant (d_{33}) was measured using a d_{33} meter (Model KCF-3500) at 110
42 Hz. The k_p was measured using an impedance analyzer PV520A (Model PV520A-T).

43 3. Result and discussion

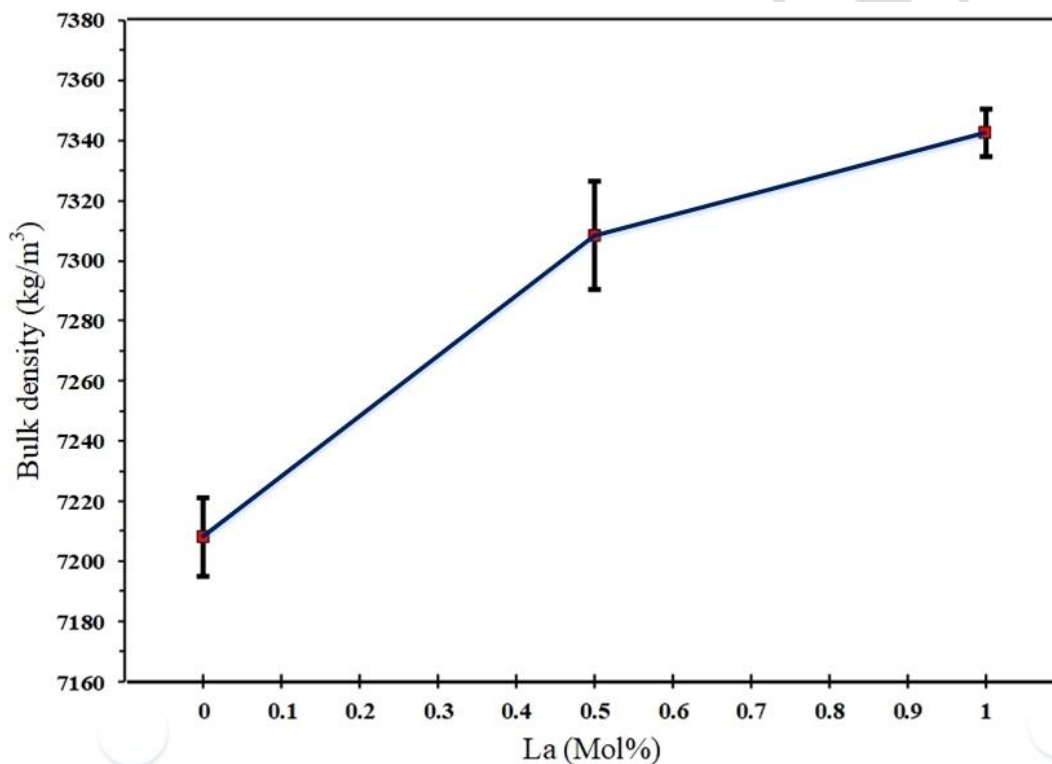
44 3.1. Sintering behavior

45 It is known that the addition of dopants substituting A- or B-site atoms can cause a
46 strong reduction of the grain size. This “grain growth inhibition effect” has been
47 attributed to the segregation of the additives in the near grain boundary region. The
48
49

1 main densification mechanism is volume diffusion, which is controlled by the number
2 of vacancies [15].

3 The La ions will substitute the Pb ions on the A site of the perovskite structure. Then
4 to conserve the electron neutrality, Pb vacancies are created, which enhance the volume
5 diffusion and consequently the final densities.

6 Fig. 1 shows the change of bulk density as a function of lanthanum content for
7 temperature investigated. As observed, the density of the samples sintered at 1280°C
8 increased with lanthanum content, with the maximum values obtained at 1.0 mol%
9 lanthanum. The optimum density of about 7340 Kg.m⁻³ was recorded for PSZTS
10 ceramics doping with 1.0 mol% lanthanum at the sintering temperature of 1280°C. The
11 results indicate that lanthanum addition could enhance the densification and reduce the
12 sintering temperature of PSZTS ceramics. This phenomenon could be explained in
13 terms of vacancy concentrations, which control the volume diffusion during
14 densification. At the thermodynamic equilibrium, a certain number of Pb vacancies
15 exist in pure materials. Impurities in the raw materials as well as those picked-up during
16 powder processing will further increase the “equilibrium” vacancy concentration.
17



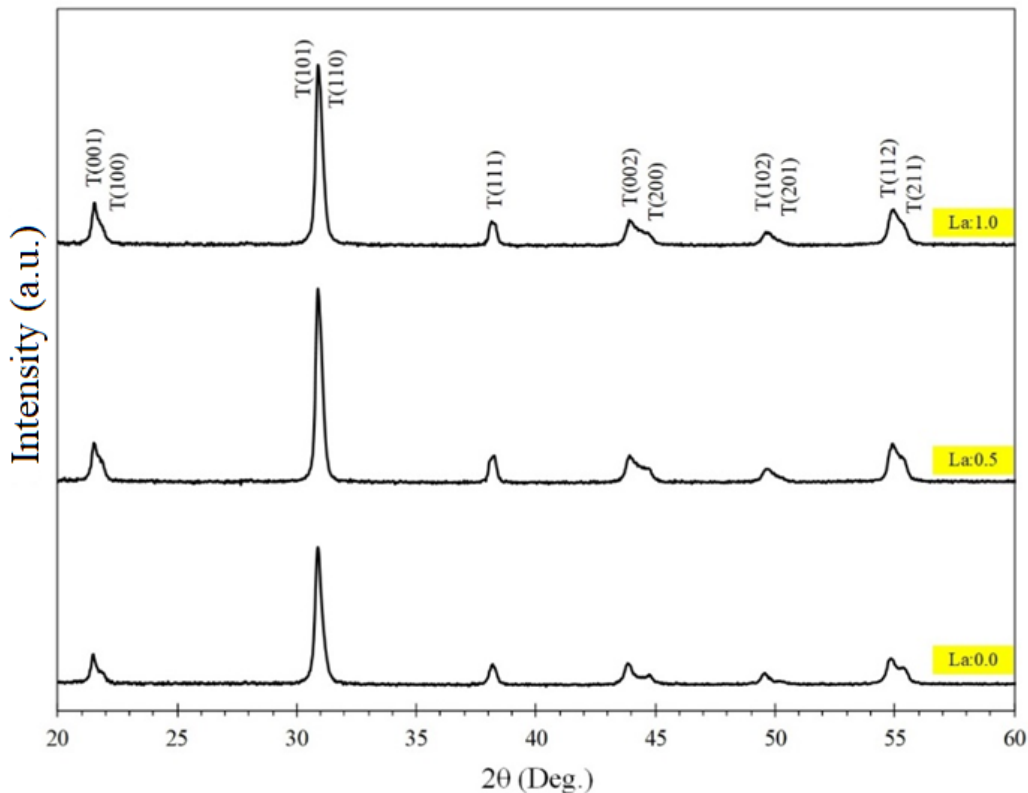
18
19 **Fig. 1. The variation of bulk density with lanthanum content at 1280°C.**

20
21 The Pb vacancy concentration in the pure PSZTS ceramics is high enough to obtain a
22 high densification rate [16] with a resulting final bulk density of 7300 Kg.m⁻³. La-doped
23 PSZTS specimens have a significant amount of Pb vacancies in order to achieve the
24 electron neutrality condition and as a consequence enhance volume diffusion and final
25 bulk density of 7340 Kg.m⁻³ (Fig. 1).
26

27 **3.2. Phase and microstructure analysis**

28 Figure 2 shows the X-ray diffraction (XRD) patterns of the composition (Pb_{0.88-}
29 _{3x/2}Sr_{0.12}La_x)(Zr_{0.54}Ti_{0.44}Sb_{0.02})O₃ for different lanthanum contents. The patterns
30 indicate the formation of the single perovskite phase. The XRD pattern of the PSZTS

1 and La-doped PSZTS samples shows the existence of the tetragonal and the
 2 rhombohedral phase. XRD results are in agreement with the literature [17, 18].
 3 Based on previous studies [18], the crystal structure should consist of a mixture of
 4 tetragonal and rhombohedral phases. As the lanthanum content increases up to 1mol %,
 5 the tetragonal phase still dominates over the rhombohedral phase.
 6 The La sites are also considered as donors, whereas Pb vacancies behave as acceptors.
 7 The La-Pb pairs can also be considered as dipoles giving rise to dipolar polarization.
 8 As the La content increases, the diffraction peak positions gradually shift toward
 9 smaller angles.
 10



11
 12 **Fig. 2. The XRD patterns of the specimens sintered at 1280°C of $(\text{Pb}_{0.88-3x/2}\text{Sr}_{0.12}\text{La}_x)(\text{Zr}_{0.54}\text{Ti}_{0.44}\text{Sb}_{0.02})\text{O}_3$ with different x values.**
 13
 14

15 The observed shift in diffraction peak position with composition can be attributed to
 16 the substitution of La^{3+} (ionic radius = 1.36 Å) for Pb^{2+} (1.49 Å) at the A-site of the
 17 perovskite lattice [19]. The smaller ionic radius of La^{3+} leads to a slight contraction of
 18 the lattice and a corresponding change in lattice parameters. In addition, due to the
 19 valence difference between La^{3+} and Pb^{2+} , charge compensation occurs via the
 20 formation of lead vacancies, which affects the local lattice distortion and structural
 21 stability. Consequently, the slight shift in peak positions indicates a minor modification
 22 of the crystal lattice, consistent with compositional variation.
 23 The X-ray diffraction (XRD) results for the samples containing 0, 0.5, and 1 mol% La
 24 are summarized in Table 1. All diffraction peaks can be indexed to a tetragonal
 25 perovskite structure with $P4mm$ symmetry, corresponding to the reflections
 26 (001)/(100), (101)/(110), (111), (002), (200), (102), and (112). No secondary phases
 27 are detected, confirming the formation of a single-phase perovskite structure. The
 28 strongest diffraction peak is observed for the (101)/(110) plane, which is typical for
 29 tetragonal PZT-based ceramics. A slight shift of the diffraction peaks toward higher 2θ
 30 values is observed with increasing La content, indicating a small change in the lattice

parameters. This shift can be attributed to the substitution of La^{3+} ions for Pb^{2+} ions at the A-site of the perovskite lattice. The calculated lattice parameters show a slight decrease in the c parameter with La doping, while the parameter changes only marginally. Consequently, the tetragonality ratio (c/a) decreases from 1.0138 for the undoped sample to 1.0106 for the sample containing 1 mol% La, suggesting a reduction in tetragonal distortion.

The theoretical density (Table 1) shows a slight variation with La addition, changing from 7840 Kg/m^3 for $x = 0$ to 7790 Kg/m^3 for $x = 0.5 \text{ mol\%}$ and 7820 Kg/m^3 for $x = 1 \text{ mol\%}$. These changes are mainly related to the small variation in unit cell volume and the decrease in formula weight due to the partial substitution of Pb by La. Overall, La incorporation slightly modifies the lattice parameters while maintaining the single-phase tetragonal perovskite structure.

Table 1. X-ray diffraction (XRD) parameters, lattice constants, and theory density calculated $(\text{Pb}_{0.87}\text{Sr}_{0.12}\text{La}_x)(\text{Zr}_{0.54}\text{Ti}_{0.44}\text{Sb}_{0.02})\text{O}_3$ ceramics.

mole%	Pos.[°2Th.]	(hkl)	Rel. Int. [%]	a	c	c/a	$\rho^{\text{theoretical}}$ (Kg/m^3)
0.0	21.57729	T (001) (100)	12.99	4.035	4.091	1.0139	7840
	30.92431	T (101) (110)	100.00				
	37.74680	T (111)	13.75				
	43.55266	T (002)	11.09				
	44.2183	T (200)	3.77				
	49.70169	T (102)	6.36				
	54.54230	T (112)	19.68				
0.5	21.59699	T (001) (100)	15.5	4.041	4.088	1.0116	7790
	30.94329	T (101) (110)	100.00				
	37.95745	T (111)	16.95				
	43.75266	T (002)	12.54				
	44.4067	T (200)	4.56				
	49.72173	T (102)	8.65				
	54.74486	T (112)	22.29				
1.0	21.627310	T (001) (100)	13.99	4.038	4.080	1.104	7820
	30.974310	T (101) (110)	100.00				
	38.257450	T (111)	14.75				
	44.052660	T (002)	13.09				
	44.706700	T (200)	4.06				
	49.750740	T (102)	7.05				
	55.044860	T (112)	21.17				

The lanthanum substitution significantly affects the microstructure of the specimens. The FESEM micrographs of the fractured surfaces of the samples sintered at 1280°C are presented in Fig. 3(a–c). The samples containing 1.0 mol% La^{3+} exhibit improved densification, which is consistent with the density measurement results. This behavior can be attributed to the donor nature of La^{3+} substitution at the A-site, which induces the formation of Pb vacancies for charge compensation, as also confirmed by XPS analysis [20]. These vacancies enhance mass transport during sintering and promote densification.

Moreover, the doped samples exhibit finer microstructures compared to the undoped composition. The reduction in grain size can be associated with the defect chemistry and vacancy concentration, which influence grain growth kinetics. The grain size distributions of the ceramics were quantitatively analyzed using Clemex Vision software, and the corresponding distribution parameters are summarized in Table 2.

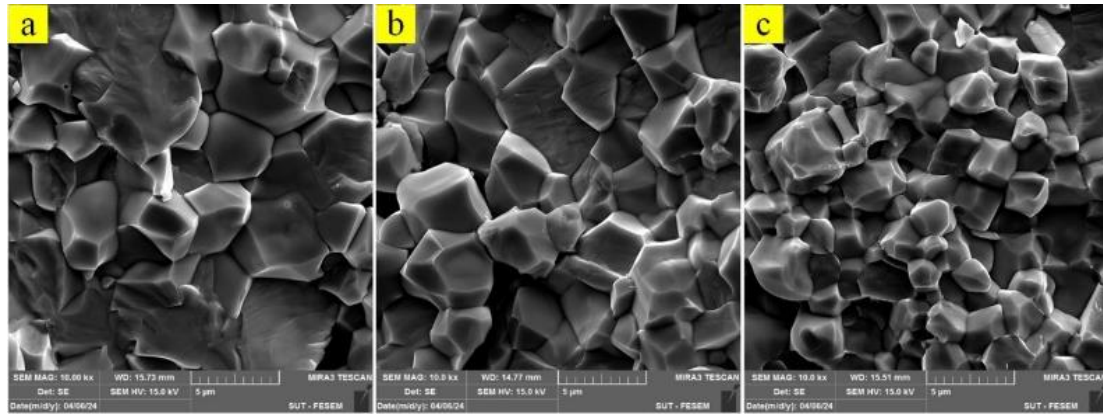


Fig. 3. The FESEM photomicrographs of the fractured surfaces of the specimens sintered at 1280°C (a) 0.0, (b) 0.5 and (c) 1.0 mole% La.

Table 2. Distribution parameters of the grain size for the different ceramics.

La mol%	Minimum (μm)	Maximum (μm)	Average (μm)	Standard deviation
0.0	1.26	5.20	2.73	1.02
0.5	0.49	5.48	2.10	0.77
1.0	0.66	3.38	1.61	0.49

The average grain size and the standard deviation for La-doped ceramics are less than that of La free ceramics. It is known that the addition of dopants substituting A- or B-site atoms can cause a strong reduction of the grain size. This “grain growth inhibition effect” has been attributed to the pinning effect of the segregated additives at the grain boundary, without any corroborating evidence as pointed out by Hammer and Hoffmann [15].

3.3. The dielectric and piezoelectric properties

Fig. 4a, b illustrates the dielectric loss and relative dielectric constant of the samples sintered at 1280°C. It is observed that increasing the lanthanum content enhanced the relative dielectric constant and the loss factor ($\tan\delta$). It is known that increasing densification causes an increase in the relative dielectric constant and a decrease in the dielectric loss as a result of the reduction in pore content. Therefore, when 1.0 mole% lanthanum was doped, the maximum value of dielectric constant and the minimum dielectric loss were obtained due to the maximum density.

Of course, the higher ϵ_r for the doped samples compared to the undoped one has also been attributed to a higher domain wall motion due to a higher Pb vacancy concentration [15]. The observed enhancement in domain wall motion is attributed to donor doping (La^{3+} and Sb^{5+}), which induces Pb vacancies for charge compensation. Unlike oxygen vacancies in acceptor-doped (hard) systems that strongly pin domain walls, Pb vacancies in donor-doped (soft) PZT systems result in reduced pinning and enhanced domain wall mobility.

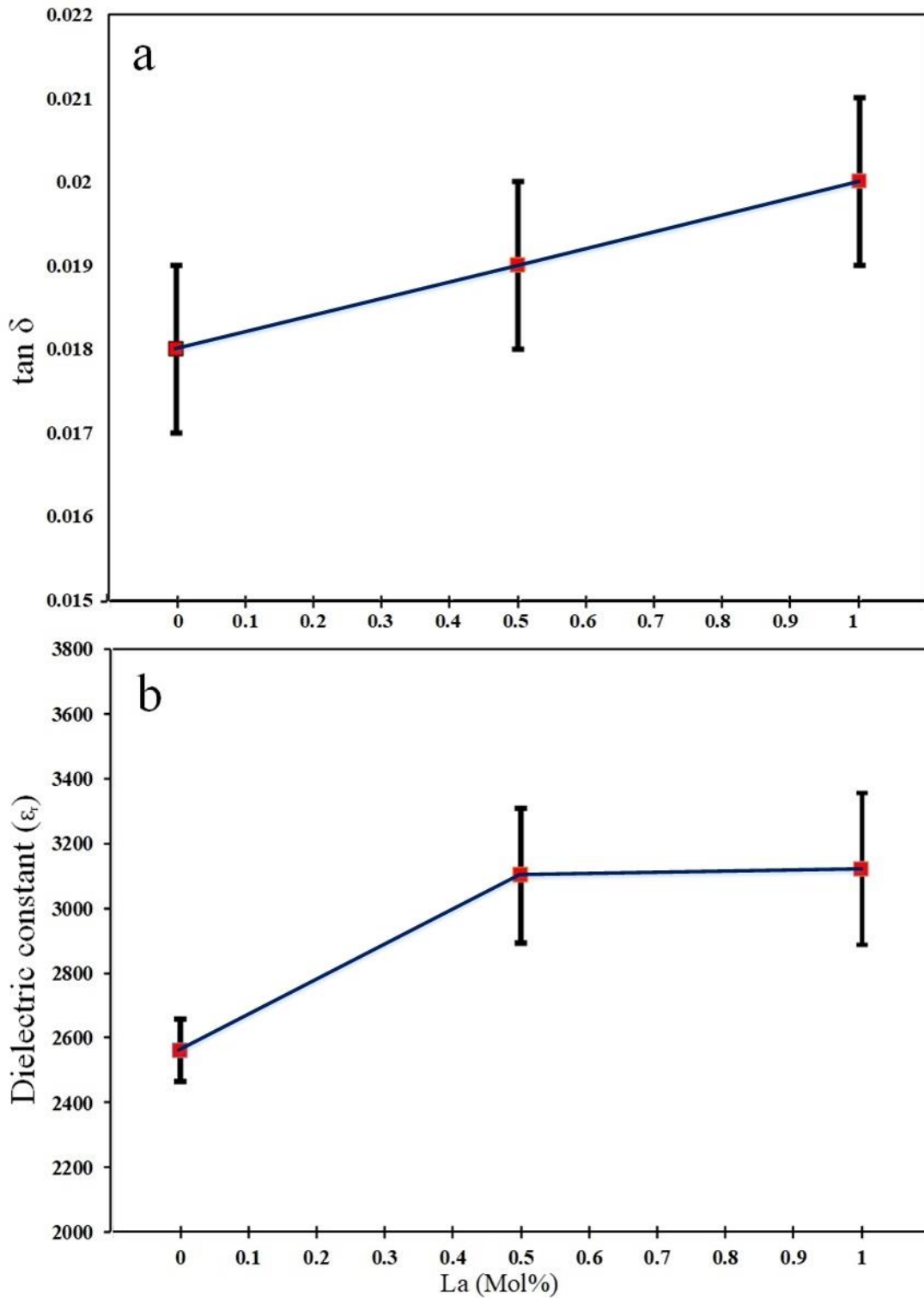


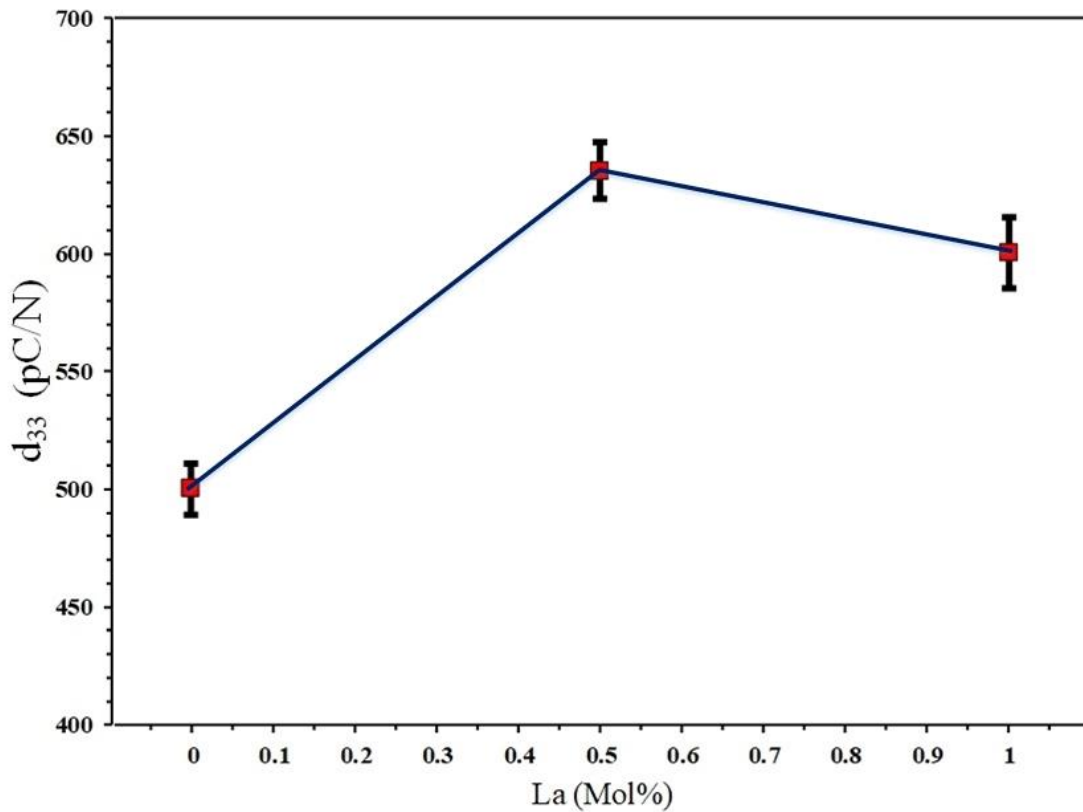
Fig. 4. The variation of (a) dielectric loss ($\tan\delta$) and (b) relative dielectric constant with lanthanum content at 1280°C.

Figures 5 and 6 show the piezoelectric coefficient d_{33} and the planar electromechanical coupling coefficient k_p for the samples sintered at 1280°C.

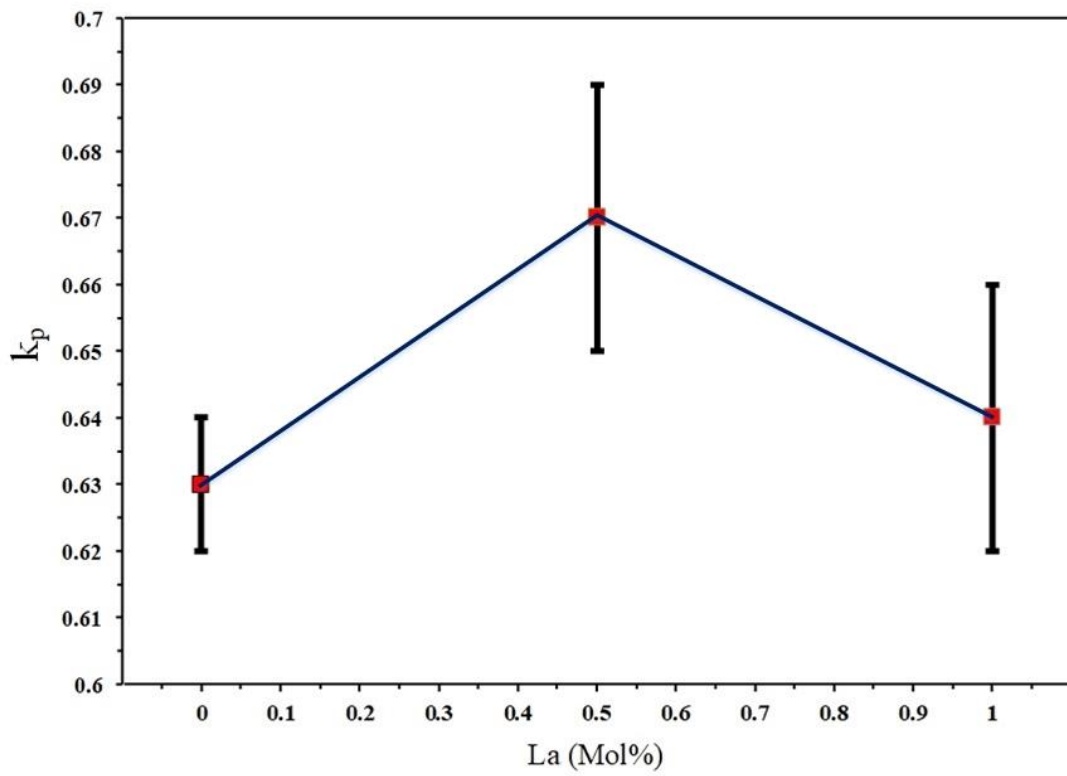
As observed, with increasing La content, the piezoelectric coefficient d_{33} and the planar electromechanical coupling k_p of the La-doped PSZTS ceramics increased greatly, reaching the maxima at 0.5 mol% La.

1
2
3
4
5
6
7
8
9

1 It is well known that La addition may control the piezoelectric, dielectric, and
2 ferroelectric properties [1]. It was revealed that La_2O_3 as a donor type dopant, enters
3 the A lattice site and thus causes Pb^{2+} vacancies in the PZT system due to the valence
4 discrepancy. Due to the increase of Pb^{2+} vacancies, the movement of the ferroelectric
5 domain walls can be promoted, which will consequently cause the drop of lattice
6 stresses, leading to the improvement of d_{33} and k_p [15]. However, with excessive
7 lanthanum addition, the excess La^{3+} ions may segregate in the grain boundaries and
8 prevent the ferroelectric domain from switching over in the process of polarization,
9 leading to the decline of d_{33} and k_p [15].
10 The maximum value of d_{33} (635 pC/N) and k_p (0.67) were obtained at 0.5 mol%
11 lanthanum content.
12



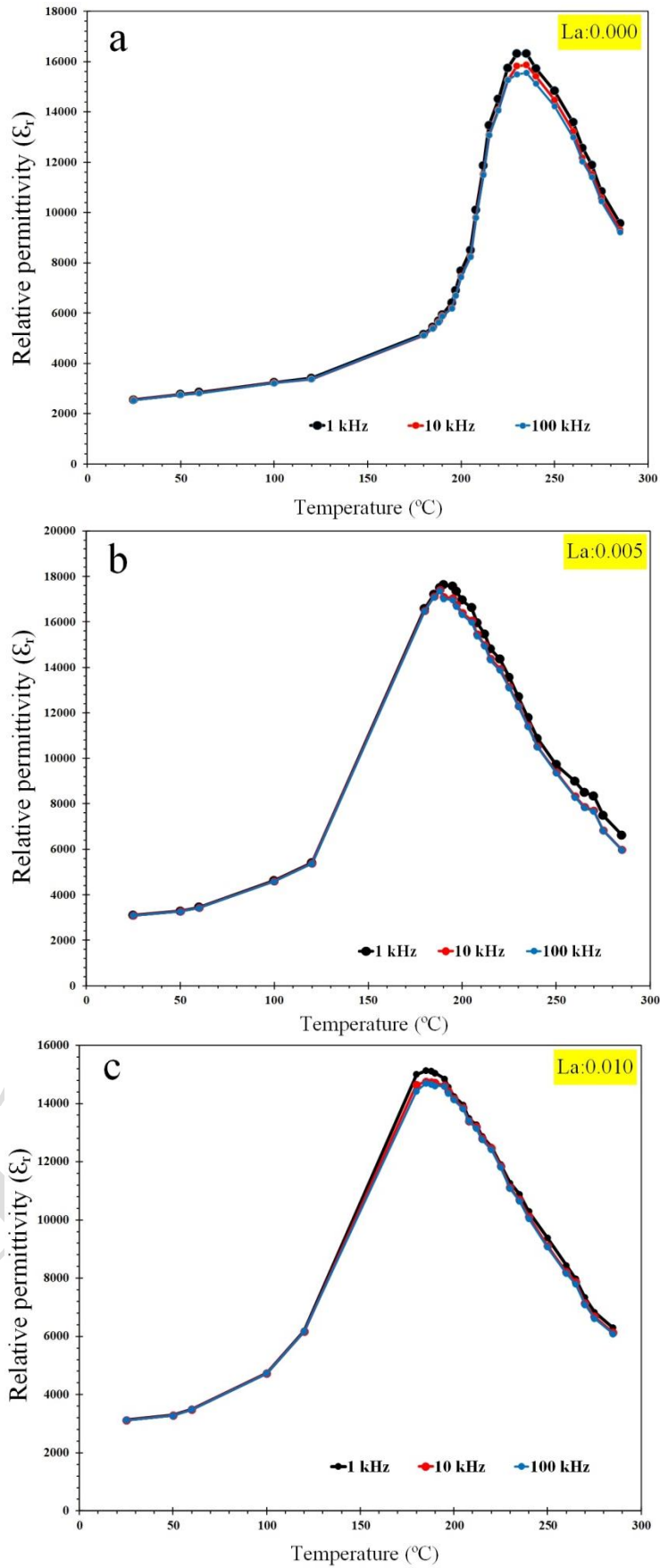
13
14 Fig. 5. The variation of the charge coefficient (d_{33}) with lanthanum content at 1280°C.
15



1
2
3
4

Fig. 6. The variation of the planar electromechanical coupling coefficient (k_p) with lanthanum content at 1280°C.

LBPI



1

2

3

4

5

6

Fig. 7. Temperature dependence of the relative permittivity (ϵ_r) for (a) $(\text{Pb}_{0.88}\text{Sr}_{0.12})(\text{Zr}_{0.54}\text{Ti}_{0.44}\text{Sb}_{0.02})\text{O}_3$ and (b) $(\text{Pb}_{0.875}\text{Sr}_{0.12}\text{La}_{0.005})(\text{Zr}_{0.54}\text{Ti}_{0.44}\text{Sb}_{0.02})\text{O}_3$ (c) $(\text{Pb}_{0.87}\text{Sr}_{0.12}\text{La}_{0.01})(\text{Zr}_{0.54}\text{Ti}_{0.44}\text{Sb}_{0.02})\text{O}_3$ ceramics, various frequencies, showing the Curie temperature.

Figure 7a (0 mol% La), b (0.5 mol% La), and c (1.0 mol% La) show the variation of relative permittivity with temperature for samples sintered at 1280 °C, measured at three frequencies: 1 kHz, 10 kHz, and 100 kHz. The Curie temperature (T_c) decreases from approximately 230 °C for the undoped sample (0 mol% La^{3+}) to about 185 °C for the sample containing 1.0 mol% La^{3+} . In addition to lowering T_c , the substitution of La^{3+} broadens the phase transition peak. Furthermore, the ϵ_r - T curves exhibit no significant shift with increasing frequency.

Table 3 compares the dielectric and piezoelectric properties of PSZTS ceramics with different dopants. In the present work, lanthanum substitution leads to improved electromechanical performance, with the optimum values obtained at 0.5 mol% La. Further increase in La content results in a decrease in d_{33} , k_p and T_C , indicating that excessive La substitution is detrimental to the overall performance.

Table 3. Comparison of the dielectric and piezoelectric properties of PSZTS ceramics doped with various elements and different La concentrations.

Dopant in PSZTS	Sintering Temperature (°C)	ϵ_r (at 1 kHz)	d_{33} pC/N	k_p	Ref.
$Pb_{0.875}Sr_{0.125}(Zr_{0.54}Ti_{0.46})O_3$	1280	1237	~240	47	[6]
$Pb_{0.875}Sr_{0.125}(Zr_{0.53}Ti_{0.47})O_3$	1280	1325	~285	51	[6]
$Pb_{0.88}Sr_{0.12}(Zr_{0.54}Ti_{0.44}Sb_{0.02})O_3$	1250	2400	527	-	[21]
$Pb_{0.88}Sr_{0.12}(Zr_{0.54}Ti_{0.44}Sb_{0.02})O_3$	1170	~2000	~600	-	[22]
$Pb_{0.88}Sr_{0.12}(Zr_{0.54}Ti_{0.44}Sb_{0.02})O_3$	1250	1479	339	66	[23]
$Pb_{0.88}Sr_{0.12}(Zr_{0.54}Ti_{0.44}Sb_{0.02})O_3$	1280	2560±96	500±11	63±1	Present paper
$Pb_{0.875}Sr_{0.12}La_{0.005}(Zr_{0.54}Ti_{0.44}Sb_{0.02})O_3$	1280	3000±209	635±12	67±2	Present paper
$Pb_{0.875}Sr_{0.12}La_{0.010}(Zr_{0.54}Ti_{0.44}Sb_{0.02})O_3$	1280	3120±236	600±15	64±2	Present paper

The results show that the incorporation of the lanthanum to the perovskite structure promotes the Pb vacancies (A site) and may likely have an intense effect on the domain motions, because of the expansion in the unit cell in the direction of the polarization [19]. The increase of the lanthanum concentration increases the A-site vacancies concentration and a higher ferroelectric domain motion [1, 16].

La substitution (>0.5 mol %) was decrease in the piezoelectric charge coefficients (d_{33}) (Fig. 5), the planar electromechanical coupling coefficient (k_p) (Fig. 6),

4. Conclusions

A significant improvement in the piezoelectric properties of $(Pb_{0.88}Sr_{0.12})(Zr_{0.54}Ti_{0.44}Sb_{0.02})O_3$ samples doped with La^{3+} was achieved. Grain size decreased with the increase of La substitution, where the highest grain size was observed in the La free composition.

The lanthanum substitution evidently promoted the density and reduced the sintering temperature of the PSZTS samples. The samples with 1.0 mol% La^{3+} addition exhibited the highest density and minimum dielectric loss at 1280°C. The samples sintered with 0.5 mol% La^{3+} additions had the optimum dielectric and piezoelectric properties. The best values of d_{33} , ϵ_r , $\tan \delta$, k_p , ρ and T_C of the samples reached the optimal values of 635 pC/N, 3000, 0.018, 0.67 and 195°C, respectively at 0.5 mol% lanthanum substitution, which are promising for pulsed transmitting transducers, high sensitivity receivers and actuators with large displacements.

References

- [1] Jaffe, B., Cook, W.R., Jaffe, H., Piezoelectric Ceramics. Academic Press, New York, 1971.

- 1 [2] Haertling, G.H., "Ferroelectric Ceramics: History and Technology", J. Am.
2 Ceram. Soc., 1999, 82, 797-818.
- 3 [3] Takahashi, S., "Effects of impurity doping in lead zirconate titanate ceramics",
4 Ferroelectrics, 1982, 41, 143-156.
- 5 [4] Moulson A.J., Herbert, J.M., *Electroceramics: Materials, Properties,*
6 *Applications*, Chapman and Hall, New York, 1990.
- 7 [5] Uchino, K., *Ferroelectric Devices*, Marcel Dekker, New York, 2000.
- 8 [6] Kulcsar, F., "Electromechanical Properties of Lead Titanate Zirconate Ceramics
9 with Lead Partially Replaced by Calcium or Strontium", J. Am. Ceram. Soc.
10 1959, 42, 343-349.
- 11 [7] Zheng, H., Reaney, I. M., Lee, W. E., Jones, N., Thomas, H., "Effects of
12 Strontium Substitution in Nb-Doped PZT Ceramics", J. Eur. Ceram. Soc., 2001,
13 21, 1371–1375.
- 14 [8] Goudarzi H., Baghshahi, S., "PZT ceramics prepared through a combined method
15 of B-site precursor and wet mechanically activated calcinate in a planetary ball
16 mill", Ceram. Int., 2017, 43, 3873–3878.
- 17 [9] Chu, S.Y., Chen, T.Y., Tsai I.T., Water, W. "Doping effects of Nb additives on
18 the piezoelectric and dielectric properties of PZT ceramics and its application on
19 SAW device", Sensor Actuators, A. 2004, 133, 198-203.
- 20 [10] Zong, X.M., Yang, Z.P., Li H., Yuan, M.B. "Effects of WO₃ addition on the
21 structure and electrical properties of Pb₃O₄ modified PZT–PFW–PMN
22 piezoelectric ceramics", Mater. Res. Bull., 2006, 41, 1447-54.
- 23 [11] Zhou, T. "The effect of doping Sb₂O₃ in high d₃₃, g₃₃ PZT Piezoelectric Ceramics",
24 Ferroelectrics, 1997, 195, 101-104.
- 25 [12] Kalem, V., Cam I., Timucin, M., "Dielectric and piezoelectric properties of PZT
26 ceramics doped with strontium and lanthanum", Ceram. Int., 2001, 37, 1265–
27 1275.
- 28 [13] Singh, V., Kumar, H.H., Kharat, D.K., Hait S., Kulkarni, M.P., "Effect of
29 Lanthanum substitution on ferroelectric properties of Niobium doped PZT
30 ceramics", Mater. Lett., 2006, 60, 2964-68.
- 31 [14] Laurent, M. Schreiner, U., Langjahr, P.A., Glazounov A.E., Hoffmann, M.J.,
32 "Microstructural and electrical characterization of La-doped PZT ceramics
33 prepared by a precursor route", J. Eur. Ceram. Soc., 2001, 21, 1495-98.
- 34 [15] Hammer M., Hoffmann, M.J., "Sintering model for mixed-oxide-derived lead
35 zirconate titanate ceramics", J. Am. Ceram. Soc., 1998, 81, 3277-3284.
- 36 [16] Gerson, R., "Variation in ferroelectric characteristics of lead zirconate titanate
37 ceramics due to minor chemical modifications", J. Appl. Phys. 31, 1960, 188-
38 194.
- 39 [17] Zheng, H., Ph.D. Thesis, Structure-property relations in Sr, Nb, Ba doped lead
40 zirconate titanate, University of Sheffield, 2001.
- 41 [18] Kalem, V., Ph.D. Thesis, Development of Piezoelectric Ceramics for Ultrasonic
42 Motor Applications, Middle East Technical University, 2011.
- 43 [19] Shannon R. D., Prewitt, C. T., "Effective ionic radii in oxides and fluorides", Acta
44 Cryst., 1970, B26, 1046.
- 45 [20] Goudarzi, H., Baghshahi, S., Tabarzadi, R., "Comparison of Dielectric and
46 Piezoelectric Properties of Sb- and Nb-Doped
47 Pb_{0.87}Sr_{0.12}La_{0.01}(Zr_{0.54}Ti_{0.44}X_{0.02})O₃ Ceramics", Ceram. Int., 2026, In press.
- 48 [21] Eitssayeam, S., Jarupoom P., Rujijanagul, G. "High Dielectric and Piezoelectric
49 Properties Observed in Annealed Pb_{0.88}Sr_{0.12}Zr_{0.54}Ti_{0.44}Sb_{0.02}O₃ Ceramics",
50 Ferroelectrics, 2013, 451, 48–53.

- 1 [22] Zheng, H., Reaney, I. M., Lee, W. E., Jones, N. Thomas, H., "Surface
2 Decomposition of Strontium-Doped Soft $\text{PbZrO}_3\text{-PbTiO}_3$ ", J. Am. Ceram. Soc.,
3 2002, 85, 207–212.
- 4 [23] Jaita, P., Kruea-In, C., Rujjanagul, G. "Influence of Al_2O_3 Nanoparticles
5 Incorporation on the Structure and Electrical Properties of
6 $\text{Pb}_{0.88}\text{Sr}_{0.12}\text{Zr}_{0.54}\text{Ti}_{0.44}\text{Sb}_{0.02}\text{O}_3$ Ceramics", Nanomaterials and Nanotechnology,
7 2016, 6, 1-7.

In Press